GEOPHYSICS, VOL. 77, NO. 2 (MARCH-APRIL 2012); P. S43–S50, 5 FIGS.
10.1190/GEO2011-0148.1

Combining full wavefield migration and full waveform inversion, a glance into the future of seismic imaging

A. J. Berkhout[1]

ABSTRACT

The next generation seismic migration and inversion technology considers multiple scattering as vital information, allowing the industry to derive significantly better reservoir models — with more detail and less uncertainty — while requiring a minimum of user intervention. Three new insights have been uncovered with respect to this fundamental transition. Unblended or blended multiple scattering can be included in the seismic migration process, and it has been proposed to formulate the imaging principle as a minimization problem. The resulting process yields angle-dependent reflectivity and is referred to as recursive full wavefield migration (WFM). The full waveform inversion process for velocity estimation can be extended to a recursive, optionally blended, anisotropic multiple-scattering algorithm. The resulting process yields angle-dependent velocity and is referred to as recursive full waveform inversion (WFI). The mathematical equations of WFM and WFI have an identical structure, but the physical meaning behind the expressions is fundamentally different. In WFM the reflection process is central, and the aim is to estimate reflection operators of the subsurface, using the up- and downgoing incident wavefields (including the codas) in each gridpoint. In WFI, however, the propagation process is central and the aim is to estimate velocity operators of the subsurface, using the total incident wavefield (sum of up- and downgoing) in each gridpoint. Angle-dependent reflectivity in WFM corresponds with angle-dependent velocity (anisotropy) in WFI. The algorithms of WFM and WFI could be joined into one automated joint migration-inversion process. In the resulting hybrid algorithm, being referred to as recursive joint migration inversion (JMI), the elaborate volume integral solution was replaced by an efficient alternative: WFM and WFI are alternately applied at each depth level, where WFM extrapolates the incident wavefields and WFI updates the velocities without any user interaction. The output of the JMI process offers an integrated picture of the subsurface in terms of angle-dependent reflectivity as well as anisotropic velocity. This two-fold output, reflectivity image and velocity model, offers new opportunities to extract accurate rock and pore properties at a fine reservoir scale.

INTRODUCTION

Until today, migration and inversion have been two different schools in analyzing seismic data. Both have a rich history in revealing subsurface information from seismic measurements, but they have different views on the problem and they use distinctly different theoretical concepts (Berkhout, 1984; Stolt and Weglein, 1985; Symes, 2008).

In seismic migration the reflectivity of geological boundaries is estimated, resulting in a structural image of the subsurface (Claerbout, 1976). This is accomplished by extrapolating source and reflected wavefields into the subsurface — using a prespecified velocity model — followed by computing, at each subsurface gridpoint, the ratio between reflected and incident wavefields. Optionally, in a next step the estimated reflectivity is transformed to elastic properties (velocity and density) of the layers between the imaged boundaries.

In seismic inversion, the elastic properties of geological layers are directly estimated, resulting in a property image of the subsurface. This is accomplished by minimizing the difference between the simulated and the recorded seismic data. Hence, forward modeling of the seismic response is central in inversion and the residue drives the iterative estimation process. Optionally, multiple scattering is included in the simulated and recorded data (Tarantola, 1987).

Manuscript received by the Editor 20 April 2011; revised manuscript received 14 August 2011; published online 27 February 2012.
[1]Delft University of Technology, Department of Geotechnology, The Netherlands. E-mail: a.j.berkhout@tudelft.nl.

Note that, in the standard practice of seismic migration, forward modeling of reflections does not take place and residues are not computed (the loop between structural image and recorded measurements is not closed). Note also that it is standard practice in migration to address primary scattering only.

In this paper, the theory of migration is extended to possibly-blended multiple-scattering wavefields, being referred to as recursive full wavefield migration (WFM). Similarly, the theory of full waveform inversion for velocity estimation is extended to recursive, optionally-blended, anisotropic, multiple scattering, being referred to as recursive full waveform inversion (WFI). New insight is given in the similarities and differences between the concepts of migration and inversion. In addition, a glimpse in the future is given by showing how the two processes can be integrated. The result is an autonomous and efficient migration-inversion process, being referred to as recursive joint migration inversion (JMI), that uses surface-related and internal multiple scattering.

EXTENDING THE MIGRATION PROCESS TO MULTIPLE SCATTERING

Standard seismic migration packages require primary reflection data as input, i.e., wavefields with a single bounce in the subsurface and thus being linear in reflectivity. This means that multiple scattering is considered as noise and need be removed prior to migration (Figure 1). WFM is proposed as the next generation migration technology. In WFM surface-related and internal multiples are included in the migration process, meaning that the wavefields in migration become nonlinear in reflectivity. It is important to realize that WFM differs fundamentally from solutions where these multiples are separately available by using a multiple prediction algorithm first (Berkhout and Verschuur, 1994; Whitmore et al. 2010) or where these multiples are "hardwired" in the process by specifying reflecting transitions in the velocity model (as can be done in reverse time migration). In WFM the input consists of a true physical dataset, the total data, and multiple handling is an integral part of the migration process.

The WFM process recursively moves down in the subsurface by downward extrapolating the incident and reflected wavefields — including multiple scattering — to each depth level z_m ($m = 1, 2, \ldots M$). The double reflectivity (representing operators for upward and downward reflection) at depth level z_m is obtained by minimizing the residue between the reflected wavefields and the weighted incident wavefields at z_m. For the next recursion (from z_m to z_{m+1}) the upward scattering generated by depth level z_m (primary + multiple tail) is subtracted from the reflection response, and the downward scattering generated by depth level z_m is added to the incident wavefields. Hence, while moving down in the subsurface, the upgoing reflected wavefield is recursively decreased and the downgoing reflected wavefield is recursively increased with higher-order reflectivity terms. When arriving at the maximum depth level ($z = z_M$), the reflection response contains the minimum number of terms (from $z \geq z_M$) and the illuminating wavefield contains the maximum number of terms: the direct source wavefield + the downward scattering of the entire overburden ($z < z_M$). In terms of mathematical equations, using the vector-matrix formulation (Berkhout, 1982), the forward WFM model for the upgoing wavefields is given by ($m = 0, 1, \ldots M-1$):

$$\vec{P}_j^-(z_m, z_0) = \sum_{n=m+1}^{M} \mathbf{W}^-(z_m, z_n)\delta\vec{P}_j(z_n, z_0) \qquad (1a)$$

and for the downgoing wavefields ($m = 1, 2, \ldots M$):

$$\vec{P}_j^+(z_m, z_0) = \mathbf{W}^+(z_m, z_0)\vec{S}_j^+(z_0) + \sum_{n=0}^{m-1} \mathbf{W}^+(z_m, z_n)\delta\vec{P}_j(z_n, z_0), \qquad (1b)$$

where $\delta\vec{P}_j(z_n, z_0)$ equals the two-way scattered wavefield generated by the gridpoints at depth level z_n, being represented by a linear combination of the up- and downgoing incident wavefields (double scattering):

$$\begin{aligned}\delta\vec{P}_j(z_n, z_0) &= \mathbf{R}^{\cup}(z_n, z_n)\vec{P}_j^+(z_n, z_0) \\ &\quad + \mathbf{R}^{\cap}(z_n, z_n)\vec{P}_j^-(z_n, z_0) \\ &= \sum_k [\vec{R}_k^{\cup}(z_n, z_n)P_{kj}^+(z_n, z_0) \\ &\quad + \vec{R}_k^{\cap}(z_n, z_n)P_{kj}^-(z_n, z_0)]. \qquad (1c)\end{aligned}$$

In equation 1c, scalars P_{kj}^+ and P_{kj}^- are respectively the downgoing and upgoing incident wavefield at gridpoint k, vectors $\vec{R}_k^{\cup}$ and $\vec{R}_k^{\cap}$ are the kth column of reflectivity matrices $\mathbf{R}^{\cup}$ and $\mathbf{R}^{\cap}$ respectively (representing angle-dependent reflection at gridpoint k) and local vector $(\vec{R}_k^{\cup}P_{kj}^+ + \vec{R}_k^{\cap}P_{kj}^-)$ being the scattered wavefield generated by gridpoint k. In equations 1a and 1b, matrices $\mathbf{W}^+$ and $\mathbf{W}^-$ define the propagation operators between two depth levels, z_0 indicates that the primary sources ($\vec{S}_j^+$) — the cause of all wavefields — are situated at the surface and j labels the source array. Hence, scalar $P_{kj}^+(z_n, z_0)$ represents the downgoing wavefield at gridpoint k of depth level z_n that was generated by source j at depth level z_0. Note that vector $\vec{S}_j^+$

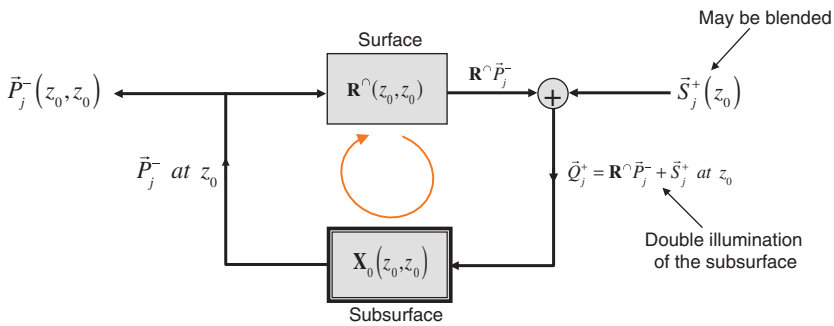

Figure 1. The feedback model, showing the up- and downgoing wavefields ($\vec{P}_j^-$ and $\vec{Q}_j^+$) at the surface (z_0). In current migration practice, the surface-related multiples have been removed from the input by preprocessing ($\vec{Q}_j^+ = \vec{S}_j^+$). In addition, internal multiples are neglected ($\vec{P}_j^+ = \mathbf{W}^+\vec{S}_j^+$), making $\mathbf{X}_0$ linear in reflectivity.

may represent a blended source array (Beasley et al., 1998), generating blended primaries and multiples.

Equation 1a, 1b, 1c shows how each gridpoint is illuminated from two sides: from above by P^+_{kj} and from below by P^-_{kj}, meaning that the total incident wavefield at gridpoint k equals $P_{kj} = P^+_{kj} + P^-_{kj}$. Equation 1a, 1b, and 1c also shows that the incident wavefields at gridpoint k (P^+_{kj}, P^-_{kj}) are weighted by the reflectivities ($\vec{R}^{\cup}_k, \vec{R}^{\cap}_k$) to generate the scattered wavefield ($\vec{R}^{\cup}_k P^+_{kj} + \vec{R}^{\cap}_k P^-_{kj}$). Note that this local vector defines a two-way wavefield (up + down) that quantifies double scattering, representing reflection and transmission effects at that gridpoint (see Figure 2). Note also that reflection and transmission are elastic processes.

Equation 1a shows that the data of a seismic shot record represents an interference pattern of upward travelling gridpoint responses ("seismic GPRs") at z_m, each GPR consisting of two components: $\mathbf{W}^- \vec{R}^{\cup}_k P^+_{kj}$ and $\mathbf{W}^- \vec{R}^{\cap}_k P^-_{kj}$, where P^+_{kj} and P^-_{kj} are the incident wavefields from above and below respectively. We will see that in WFM both wavefield components are used to estimate the reflection operators at gridpoint k.

In equation 1b the first term $\mathbf{W}^+ \vec{S}^+_j$ represents illumination at z_m by the direct wavefield from the primary source distribution at z_0. In the second term, the expressions $\mathbf{W}^+ \vec{R}^{\cap}_k P^-_{kj}$ and $\mathbf{W}^+ \vec{R}^{\cup}_k P^+_{kj}$ represent the extra illumination by the downward scattering from each secondary source k at depth level z_n, where $n = 0, 1, 2, \ldots m-1$. Again, we will see that in WFM all three wavefield components are taken into account to obtain the full illuminating wavefield at gridpoint k.

In summary, equation 1a, 1b, and 1c shows that wavefield propagation in an inhomogeneous medium can be described by a linear superposition (weighted sum) of direct and scattered wavefields that travel in an inhomogeneous smooth (optionally scatter-free) medium, the propagation operators of this medium being given by $\mathbf{W}^+$ (down) and $\mathbf{W}^-$ (up). The direct wavefield is generated by primary sources at the acquisition surface ($\mathbf{W}^+ \vec{S}^+_j$) and the scattered wavefields are generated by secondary sources in the subsurface at the inhomogeneous gridpoints given by $\sum \mathbf{W}^+ \delta \vec{P}_j$ (down) and $\sum \mathbf{W}^- \delta \vec{P}_j$ (up). Note that P^-_{kj} and P^+_{kj}, and thus $\delta \vec{P}_j$, are nonlinear in reflectivity.

Forward modeling equation 1a, 1b, and 1c can be applied in an iterative way, alternately updating P^+_{kj} and P^-_{kj}, starting with the linear solution $\vec{P}^+_j = \mathbf{W}^+ \vec{S}^+_j$ and $\vec{P}^-_j = [\mathbf{W}^- \mathbf{R}^{\cup} \mathbf{W}^+] \vec{S}^+_j$, until the highest required order of multiple scattering is obtained. In this paper, we are not interested in modeling but we focus on migration and inversion, meaning that measurements are given and the subsurface is unknown. In the standard practice of current migration the multiple scattering process is neglected, meaning that in the wavefield model the second term in equation 1b and 1c is neglected (no multiple reflection and no transmission effects) and gridpoint reflectivity vector $\vec{R}^{\cup}_k$ is estimated only (Figure 1). In WFM, however, both terms in equation 1b and c are used and both gridpoint reflectivity vectors $\vec{R}^{\cup}_k$ and $\vec{R}^{\cap}_k$ are estimated. Note that if we neglect angle dependence, then $\mathbf{R}^{\cup}$ and $\mathbf{R}^{\cap}$ become diagonal matrices and the reflectivity vectors simplify to the scaled unity vectors $\vec{R}^{\cup}_{kk}$ and $\vec{R}^{\cap}_{kk}$, containing angle-averaged reflection coefficients $R^{\cup}_{kk}$ and $R^{\cap}_{kk}$ only.

In WFM, the unknown reflectivities ($\vec{R}^{\cup}_k$ and $\vec{R}^{\cap}_k$) are found by the following constrained minimization process at the surface (z_0):

$$\vec{P}^-_j(z_0, z_0) - \sum_{m=1}^{M} \mathbf{W}^-(z_0, z_m) \delta \vec{P}_j(z_m, z_0) = \text{minimum for all } j, \tag{2a}$$

where

$$\begin{aligned} \delta \vec{P}_j(z_m, z_0) &= \mathbf{R}^{\cup}(z_m, z_m) \vec{P}^+_j(z_m, z_0) \\ &\quad + \mathbf{R}^{\cap}(z_m, z_m) \vec{P}^-_j(z_m, z_0) \\ &= \sum_k [\vec{R}^{\cup}_k(z_m, z_m) P^+_{kj}(z_m, z_0) \\ &\quad + \vec{R}^{\cap}_k(z_m, z_m) P^-_{kj}(z_m, z_0)], \end{aligned} \tag{2b}$$

the constraint imposing that the reflectivities are not allowed to contain traveltimes.

To avoid dealing with a complex iterative problem, solving a volume integral equation of the second kind, we follow today's migration technology and make recursive downward extrapolation part of the solution:

$$\vec{Q}^-_j(z_m, z_0) = \mathbf{W}^*(z_m, z_{m-1}) \vec{P}^-_j(z_{m-1}, z_0), \tag{3a}$$

$$\vec{P}^+_j(z_m, z_0) = \mathbf{W}^+(z_m, z_{m-1}) \vec{Q}^+_j(z_{m-1}, z_0), \tag{3b}$$

where $\mathbf{W}^*(z_m, z_{m-1})$ is the conjugate complex version of propagation operator $\mathbf{W}^+(z_m, z_{m-1})$. Note the difference between the wavefields $\vec{P}$ and $\vec{Q}$: $\vec{P}$ refers to the incident wavefield at depth level z_m and $\vec{Q}$ includes the response of depth level z_m. Next, constrained minimization is applied at depth level z_m for all shot records (all j):

$$\mathbf{Q}^-(z_m, z_0) - \mathbf{R}^{\cup}(z_m, z_m) \mathbf{P}^+(z_m, z_0) - \mathbf{R}^{\cap}(z_m, z_m) \mathbf{P}^-(z_m, z_0) = \textit{minimum} \tag{4a}$$

or, applying the linear Radon transform to the receiver coordinates at z_m (Berkhout, 1997):

$$\tilde{\mathbf{Q}}^-(z_m, z_0) - \tilde{R}^{\cup}(z_m, z_m) \mathbf{P}^+(z_m, z_0) - \tilde{R}^{\cap}(z_m, z_m) \mathbf{P}^-(z_m, z_0) = \textit{minimum}, \tag{4b}$$

each column of $\tilde{\mathbf{R}}^{\cup}$ and $\tilde{\mathbf{R}}^{\cap}$ representing the angle-dependent reflection coefficients at gridpoint k. Equation 4a and 4b show that the

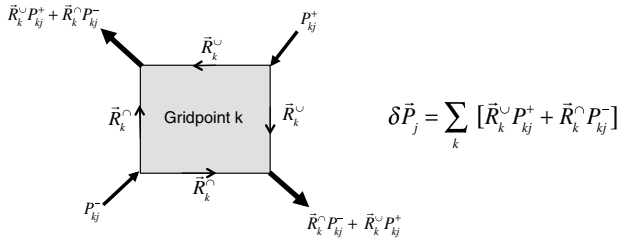

Figure 2. The scattered wavefield at gridpoint k equals a linear combination of the incident wavefields ($\vec{P}^-_j, \vec{P}^+_j$), quantifying reflection and transmission. Note that any scattered wavefield is two-way and spatially continuous.

complex 3D problem in equation 2a has been reduced to M relatively simple 2D problems!

Equation 4a and 4b means that the scattered wavefields generated at z_m, denoted by $\delta\vec{P}_j$, are removed from the total upgoing wavefield ($\vec{Q}_j^-$) at z_m in a data-adaptive manner in all shot records (all j). The residue equals the upgoing wavefield without the scattered wavefield at z_m, leading to incident upgoing wavefield $\vec{P}_j^-$:

$$\vec{P}_j^-(z_m, z_0) = \vec{Q}_j^-(z_m, z_0) - \delta\vec{P}_j(z_m, z_0) \quad \text{for } m = 1, 2, \ldots M. \tag{5a}$$

Next, the scattered wavefield ($\delta\vec{P}_j$) is added to the downgoing wavefield ($\vec{P}_j^+$) at z_m, leading to extended illumination (typical for WFM):

$$\vec{Q}_j^+(z_m, z_0) = \vec{P}_j^+(z_m, z_0) + \delta\vec{P}_j(z_m, z_0) \quad \text{for } m = 1, 2, \ldots M. \tag{5b}$$

Figure 3 shows the computational diagram.

Note that it is standard practice in migration to ignore $\mathbf{R}^\cap$, meaning that $\vec{P}_j^+ = \mathbf{W}^+\vec{S}_j^+$ and $\delta\vec{P}_j = \mathbf{R}^\cup\vec{P}_j^+$ only (multiple scattering is considered to be shot generated noise). Note also that in the structural version of WFM minimization 4b is carried out for the scalars $\tilde{R}_{kk}^\cup$ and $\tilde{R}_{kk}^\cap$ only (normal incidence), and physics tells us that we may write $\tilde{R}_{kk}^\cap = -\tilde{R}_{kk}^\cup$. This fundamental condition is included as an extra constraint in minimization process 4b: $\tilde{R}_{kk}^\cup + \tilde{R}_{kk}^\cap = minimum$. Note that in the acoustic situation (no mode conversion), the condition may be extended to $\vec{R}_k^\cap = -\vec{R}_k^\cup$, meaning that in the acoustic version of WFM:

$$\delta\vec{P}_j = \mathbf{R}^\cup(\vec{P}_j^+ - \vec{P}_j^-) = \mathbf{R}^\cap(\vec{P}_j^- - \vec{P}_j^+). \tag{6}$$

If operators $\mathbf{W}^+$ and $\mathbf{W}^-$ address the propagation of P-waves only, $\mathbf{R}^\cup$ and $\mathbf{R}^\cup$ represent P-P reflection (of course in a full elastic sense). This means that the WFM residue contains converted waves that may be addressed in a second minimization step, etc.

While moving down in the subsurface ($m = 1, 2, \ldots M$), it is well known that primary reflections become weaker, but it is not always realized that the energy of the coda will increase. In today's migration algorithms, codas are not addressed and this may be the reason that deep data — particularly below highly reflective overburdens — cannot be properly imaged, even with perfect velocities. In WFM, however, codas generated by reflectors in the overburden ($z \le z_m$) are included in the wavefield model, creating two major advantages. First, codas are subtracted from the response ($\vec{Q}_j^-$) of the deeper reflectors, decreasing the interference effects in the deep data (equation 5a). Second, codas are not only removed from $\vec{Q}_j^-$; they are also included in $\vec{P}_j^+$ to enhance the illuminating wavefield, allowing better estimates of the reflectivity (equation 5b), particularly for deep horizons in shadow zones.

EXTENDING FULL WAVEFORM INVERSION TO THE FULL SEISMIC BANDWIDTH

In the last few years we have seen the development of full waveform inversion (FWI) algorithms to estimate low wave-number velocity models for migration purposes. In these algorithms, the low-frequency seismic response is numerically simulated by acoustic finite difference modeling (typically up to 15–20 Hz) and compared with the low-frequency version of the recorded measurements. By updating the velocity model, using some gradient-driven optimization algorithm, the simulated data is updated until it

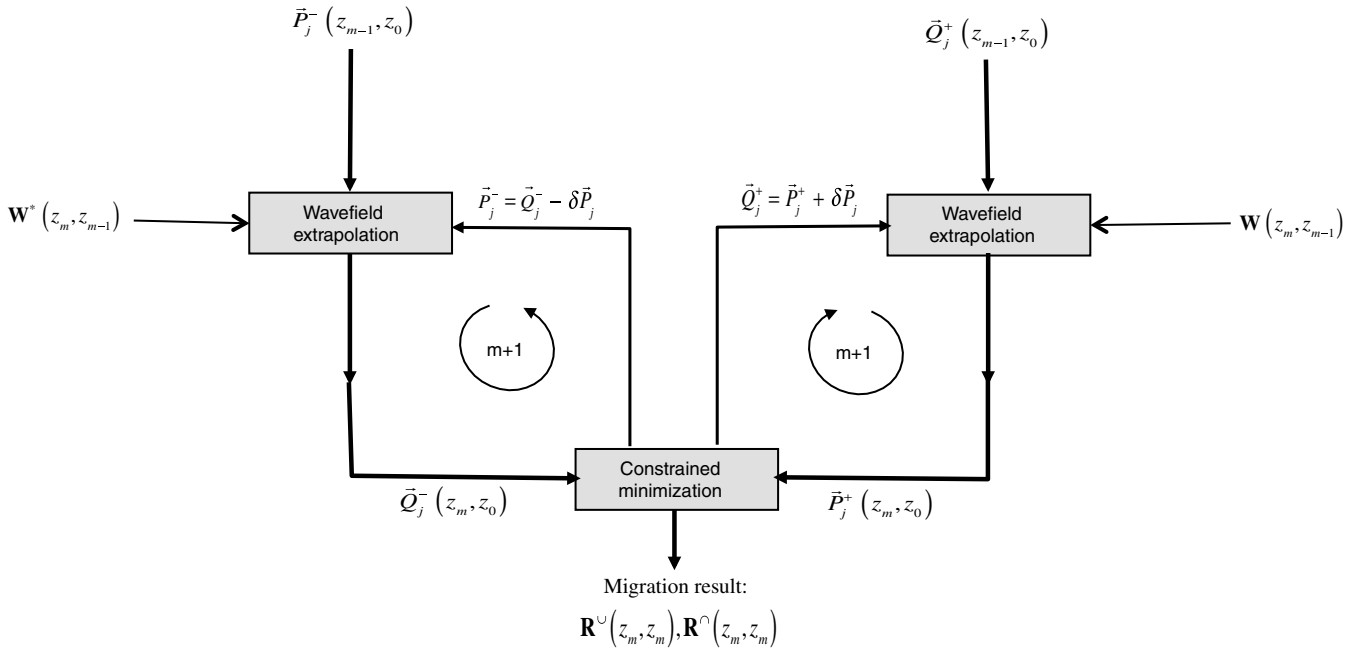

Figure 3. In the recursive process of WFM, reflectivity matrices $\mathbf{R}^\cup$ and $\mathbf{R}^\cap$ are computed by adaptively subtracting scattered wavefield $\delta\vec{P}_j$ from response $\vec{Q}_j^-$ for each depth level (constrained minimization), yielding residue $\vec{P}_j^-$. In addition, the illuminating wavefield is updated by adding $\delta\vec{P}_j$ to $\vec{P}_j^+$, yielding $\vec{Q}_j^+$. In practice, minimization is simultaneously carried out for several depth levels around z_m.

matches the recorded measurements (see overview Virieux and Operto, 2009). As expected, large offsets play an important role in the updating process. We observe that these iterative, low-frequency FWI algorithms increasingly compliment the traditional migration-velocity analysis packages.

Today, we see a new development at the horizon: FWI algorithms are being extended to the high end of the seismic bandwidth (say 100 Hz) by abandoning the time consuming finite difference simulation of wavefields. Instead, an elastic background model is introduced, and the difference between the known elastic background properties and the unknown real medium properties, called the spatial contrast function, is inverted for. There is already a wealth of publications on this approach in the seismic and electromagnetic literature. See for instance Zhdanov, 2002; Abubakar et al., 2009; Gisolf and Verschuur, 2010. At each gridpoint, the contrast acts as a point scatterer in the background medium, generally referred to as a "contrast source" (see above references). Note that if we invert for P-wave velocity only and we ignore anisotropy, then this contrast source represents a monopole. The total wavefield in the true medium equals the sum of the wavefields of the primary sources in the background (background wavefield) and the wavefield of all point scatterers in the background (differential wavefield). Hence, by choosing a simple background the subsurface detail is not hardwired in the solution and the wavefield simulation process is relatively simple and very efficient. For instance, in a smooth background medium, the background wavefield equals the direct source wavefield only. In FWI, the contrasts and the total wavefield are alternately updated until the total simulated wavefield matches the recorded wavefield at the detector positions. In terms of mathematical equations, using again the vector-matrix formulation, the forward model of FWI is given by ($m = 0, 1, 2, \ldots M$):

$$\vec{P}_j(z_m, z_0) = \mathbf{G}_0(z_m, z_0)\vec{S}_j(z_0) + \sum_{n=1}^{M} \mathbf{G}_0(z_m, z_n)\delta\vec{P}_j(z_n, z_0), \tag{7a}$$

where

$$\delta\vec{P}_j(z_n, z_0) = \sum_k \vec{\chi}_{kk}(z_n, z_n)P_{kj}(z_n, z_0) \tag{7b}$$

represents the contrast sources at depth level z_n.

In equation 7a, vector $\vec{S}_j(z_0)$ represents a distribution of primary sources in terms of monopoles at the reflection-free acquisition surface z_0, vector $\vec{P}_j$ represents the total incident wavefield at depth level z_m, $(\vec{P}_j^+ + \vec{P}_j^-)$, matrix $\mathbf{G}_0$ represents the simple background Green's function between two depth levels, and vector $\delta\vec{P}_j(z_n, z_0)$ is the scattered wavefield at depth level z_n. In equation 7b, vector $\vec{\chi}_{kk}$ equals a scaled unity vector with element χ_{kk}, and scalar χ_{kk} represents the contrast property at gridpoint k. If inversion occurs for P-wave velocities only (the focus of this paper), we may write: $\chi_{kk} = (\omega^2/c_k^2 - \omega^2/c_{0,k}^2)$, where $c_{0,k}$ equals the background velocity in gridpoint k. It is important to realize that if we neglect the second term in equation 7a, then $\vec{P}_j = \vec{P}_j^+$ equals the downgoing source wavefield only and in equation 7b, $\delta\vec{P}_j = \delta\vec{P}_j^-$ equals the upgoing scattered wavefield that is linear in χ_{kk} (Born approximation). For details the reader is referred to Zhdanov (2002).

In the following, basic equation 7a and 7b is extended to the situation with a reflective surface, meaning that surface-related multiples are included:

$$\vec{P}_j(z_m, z_0) = \mathbf{W}_0(z_m, z_0)\vec{Q}_j^+(z_0) + \sum_{n=1}^{M} \mathbf{G}_0(z_m, z_n)\sum_k \vec{\chi}_{kk}(z_n, z_n)P_{kj}(z_n, z_0), \tag{8a}$$

where (see again Figure 1)

$$\vec{Q}_j^+(z_0, z_0) = \vec{S}(z_0) + \mathbf{R}^{\cap}(z_0, z_0)\vec{P}_j^-(z_0, z_0). \tag{8b}$$

In equation 8a, matrix $\mathbf{W}_0$ represents the background propagation operator between two depth levels ($\mathbf{W}_0 = \partial_{z_0}\mathbf{G}_0$), vector $\mathbf{W}_0\vec{Q}_j^+$ represents the background wavefield (generated by the primary and secondary sources at z_0) and the sum of seismic GPRs from all depth levels, $\sum_n \mathbf{G}_0\delta\vec{P}_j$, equals the differential wavefield ($\delta\vec{P}_j$ (being generated by the contrast sources $\vec{\chi}_{kk}P_{kj}$ at depth level z_n). In equation 8b vector $\vec{S}_j^+$ represents a distribution of primary sources in terms of dipoles and $\mathbf{R}^{\cap}\vec{P}_j^-$ equals the distribution of secondary sources, again in terms of dipoles, at the reflective acquisition surface z_0. Equation 8b shows that for a reflective surface the subsurface is illuminated by two wavefields (double illumination), where the primary sources may be arranged in a blended array.

In the FWI process for velocity estimation, measurements are given and the velocity contrast function is estimated in an iterative manner. This is done by (a) applying an inversion step at acquisition surface z_0:

$$\vec{P}_j(z_0, z_0) - \sum_{m=1}^{M} \mathbf{G}_0(z_0, z_m)\delta\vec{P}_j(z_m, z_0) = \text{minimum for all } j \tag{9a}$$

with

$$\delta\vec{P}_j(z_m, z_0) = \sum_k \vec{\chi}_{kk}(z_m, z_m)P_{kj}(z_m, z_0), \tag{9b}$$

yielding an update of scalar χ_{kk} at each subsurface gridpoint, and (b) by applying an iterative modeling step (double sum of the seismic GPRs):

$$\Delta\vec{P}_j(z_m, z_0) = \sum_{n=1}^{M} \mathbf{G}_0(z_m, z_n)\delta\vec{P}_j(z_n, z_0) = \sum_{n=1}^{M} \mathbf{G}_0(z_m, z_n)\sum_k \vec{\chi}_{kk}(z_n, z_n)P_{kj}(z_n, z_0) \quad \text{for } m = 0, 1, \ldots\ldots\ldots M-1, \tag{10a}$$

yielding an update of the total incident wavefield:

$$\vec{P}_j(z_m, z_0) = \mathbf{W}_0(z_m, z_0)\vec{Q}_j^+(z_0) + \Delta\vec{P}_j(z_m, z_0) \tag{10b}$$

at each depth level. Note that the iterative process starts by taking $\vec{P}_j = \mathbf{W}_0\vec{Q}_j^+$ in inversion step 9a, meaning that we start with a zero differential wavefield ($\Delta\vec{P}_j = 0$). This Born inversion step leads to the first estimate of scalar χ_{kk} in each gridpoint, followed by updating $\vec{P}_j$, etc. (Figure 4). It is important to realize that this inversion process is very elaborate as it solves a volume integral equation of the second kind (Zhdanov, 2002; Abubakar et al., 2009). Later in

this paper, I will propose a recursive alternative, referred to as WFI, that is based on solving the integral equation per depth layer.

COMPARING FWM WITH FWI

In WFM, seismic reflection measurements are described by the combined responses of secondary sources (GPRs). These sources are situated in the gridpoints of a user-specified medium, the velocity distribution of this medium defining an accurate estimate of the actual propagation operators $\mathbf{W}^+$ and $\mathbf{W}^-$. Each gridpoint source has a signature that is given by the incident wavefields (P^+_{kj}, P^-_{kj}) and its directional strength is determined by the angle-dependent reflectivities at that gridpoint ($\vec{R}^{\cup}_k$, $\vec{R}^{\cap}_k$), yielding the scattered wavefield generated by that gridpoint: $\vec{R}^{\cup}_k P^+_{kj} + \vec{R}^{\cap}_k P^-_{kj}$. Incident wavefields ($P^+_{kj}$, P^-_{kj}) are computed by recursive downward extrapolation.

In FWI seismic reflection measurements are also described by responses of secondary sources (GPRs). But unlike migration, the point sources are now situated in the gridpoints of a background medium with a prespecified — preferably smooth — velocity distribution. In addition, the signature of each gridpoint source (or contrast source) is given by the total incident wavefield ($P^+_{kj} + P^-_{kj}$) and its omnidirectional strength is determined by the difference between the true and the background velocity distribution ($\vec{\chi}_{kk}$) at that gridpoint, yielding the scattered wavefield generated by that gridpoint: $\vec{\chi}_{kk}(P^+_{kj} + P^-_{kj})$. In FWI, the true subsurface (in terms of velocity) is found by estimating the total incident wavefield at each gridpoint (P_{kj}) with the aid of forward modeling, followed by determining the contrasts ($\vec{\chi}_k$) by minimizing the difference between the combined GPRs — representing the modeled measurements — and the true measurements at the acquisition surface. Because the total incident wavefield at each gridpoint is also determined by the GPRs of the other gridpoints — representing internal multiple scattering — the total procedure, modeling and minimization, must be carried out in an iterative way (Figure 4).

In summary, WFM and FWI use multiple scattering, and they both close the loop between output and input. However, in WFM the subsurface is described in terms of gridpoint reflectivities, and in FWI the subsurface is described in terms of gridpoint contrasts. Moreover, in WFM wavefields (up, down) are computed by recursive wavefield extrapolation, and in FWI wavefields (up + down) are computed by a nonrecursive, iterative wavefield modeling process. Last but not least, in WFM the gridpoint sources define physical scatterers at all locations where reflecting boundaries occur. I refer to these physical scatterers as "***A***-scatterers"; they address the difference in amplitude between the incident and reflected wavefields. Errors in the traveltimes (caused by erroneous velocities) are not corrected for and, therefore, they cause errors in the reflectivity. In FWI, the gridpoint sources define virtual scatterers at all locations where background and true medium are different. I refer to these mathematical scatterers as "***B***-scatterers"; they are able to address the difference in traveltime between the wavefields in the background and the true medium. Hence, WFM and FWI are complementary processes that use the amplitude and phase information in the seismic data respectively.

To illustrate the above, let us consider a constant velocity medium with one reflector due to a density change (note that there is no physical multiple scattering in this example). In the forward model of WFM, this medium is represented by propagation operators ($\mathbf{W}^+$, $\mathbf{W}^-$) and scatterers are only positioned at the gridpoints of the reflector to represent a physical scattering process at those gridpoints. In the forward model of FWI, the situation is very different: the medium is represented by background operators ($\mathbf{W}_0$,$\mathbf{G}_0$) and scatterers are positioned at every gridpoint of the medium to represent a complex virtual scattering process everywhere in the homogeneous layer.

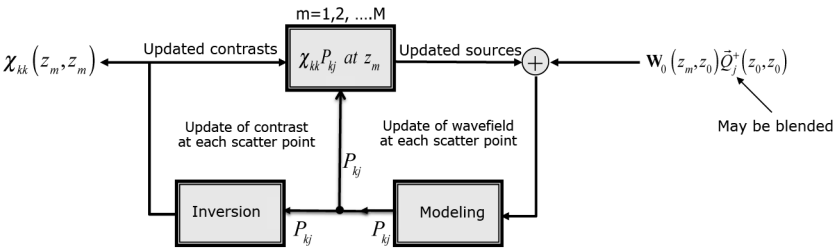

Figure 4. In the broadband implementation of FWI, a complex volume integral equation is iteratively solved. Total wavefield P_{kj} and contrast scalar χ_{kk} are alternately updated until the simulated wavefield matches the recorded wavefield at the detector positions.

A GLIMPSE IN THE FUTURE OF SEISMIC IMAGING

A major problem in migration is the specification of a velocity distribution that yields an accurate representation of propagation operators $\mathbf{W}^+$ and $\mathbf{W}^-$ used in the wavefield extrapolation processes. If we consider the migration velocity distribution as a background velocity model, then WFM and the recursive version of FWI can be combined into one automated joint migration-inversion process. This combination, recursive, joint migration-inversion (JMI), yields an accurate reflectivity image as well as an accurate velocity model without any user interaction. With reference to equations 2a and 9a, we may write for the two combined minimization processes of JMI at depth level z_m (single level formulation):

$$\mathbf{Q}^-(z_m,z_0) - [\mathbf{U}(z_m,z_m)\mathbf{P}^+(z_m,z_0) + \mathbf{V}(z_m,z_m)\mathbf{P}^-(z_m,z_0)] = minimum, \tag{11a}$$

where the input wavefields for the minimization are obtained by recursive downward extrapolation (see equation 3a and 3b) and where matrices $\mathbf{U}$ and $\mathbf{V}$ are the unknowns at z_m. In the WFM process, the matrices $\mathbf{U}$ and $\mathbf{V}$ represent the reflectivity vectors:

$$\mathbf{U}(z_m,z_m) = (\vec{R}^{\cup}_1, \vec{R}^{\cup}_1, \ldots\ldots \vec{R}^{\cup}_k \ldots\ldots) \quad \text{and}$$
$$\mathbf{V}(z_m,z_m) = (\vec{R}^{\cap}_1, \vec{R}^{\cap}_1, \ldots\ldots \vec{R}^{\cap}_k \ldots\ldots), \tag{11b}$$

and in the WFI process for velocity estimation, the matrices $\mathbf{U}$ and $\mathbf{V}$ are equal, representing the contrast vectors:

$$\mathbf{U}(z_m,z_m) = \mathbf{V}(z_m,z_m) = (\vec{\chi}_1, \vec{\chi}_2, \ldots\ldots\ldots \vec{\chi}_k, \ldots\ldots\ldots). \tag{11c}$$

Note that equation 11a states that multiple scattering is linear in the incident wavefields, meaning that the physical and virtual multiple

scattering wavefields obey the wave equation for any inhomogeneous subsurface (no prior assumptions). In equation 11c, therefore, single-element contrast vector $\vec{\chi}_{kk}$ (containing scalar χ_{kk} only) can be generalized by the multi-element contrast vector $\vec{\chi}_k$. Similar to the well-known representation of reflectivity (Berkhout, 1982) — where single-element vector $\vec{R}_{kk}$ (containing scalar R_{kk} only) represents angle-averaged reflection and multi-element vector $\vec{R}_k$ represents angle-dependent reflection at gridpoint k — single-element vector $\vec{\chi}_{kk}$ represents angle-averaged velocity and multi-element vector $\vec{\chi}_k$ represents the angle-dependent velocity at gridpoint k.

In the JMI process full wavefield extrapolation is applied from z_{m-1} to z_m first, using the wavefields $\vec{Q}_j^+$ and $\vec{P}_j^-$ at depth level z_{m-1} according to extrapolation equation 3a and 3b. This extrapolation step yields an estimate of the total wavefield, being denoted by $< \vec{P}_j >$, at intermediate depth levels z_n ($z_{m-1} < z_n \le z_m$):

$$< \vec{P}_j(z_n, z_0) > = \mathbf{W}_0(z_n, z_{m-1})\vec{Q}_j^+(z_{m-1}, z_0) + \mathbf{W}_0^*(z_n, z_{m-1})\vec{P}_j^-(z_{m-1}, z_0).$$

Next, a full waveform inversion step is applied: the estimated wavefields at z_n are used to compute the exact total wavefields $\vec{P}_j$ as well as the contrast vectors $\vec{\chi}_k$ by using equation 8a:

$$\vec{P}_j(z_n, z_0) = < \vec{P}_j(z_n, z_0) > + \Delta\vec{P}_j(z_n, z_0) \quad \text{with}$$
$$\Delta\vec{P}_j(z_n, z_0) = \sum_{l=m-1}^{m} \mathbf{G}_0(z_n, z_l) \sum_k \vec{\chi}_k(z_l, z_l) P_{kj}(z_l, z_0), \quad (12)$$

yielding an update of the velocities (including anisotropy) in each gridpoint of layer (z_{m-1}, z_m) and an update of the wavefields at z_m:

$$\vec{P}_j^+(z_m, z_0) = \mathbf{W}_0(z_m, z_{m-1})\vec{Q}_j^+(z_{m-1}, z_0) + \Delta\vec{P}_j(z_m, z_0)$$
$$\vec{Q}_j^-(z_m, z_0) = \mathbf{W}_0^*(z_m, z_{m-1})\vec{P}_j^-(z_{m-1}, z_0) - \Delta\vec{P}_j(z_{m-1}, z_0). \quad (13)$$

After completion, the updated velocities in layer (z_{m-1}, z_m) as well as the reflectivities and updated wavefields at depth level z_m are known, and we are ready to move down by applying the following full wavefield extrapolation step (from z_m to z_{m+1}) and the following full waveform inversion step (between z_m and z_{m+1}), etc. Note that the JMI process works with two different scales: In the order of tens of meters, say 50 m, in the migration step (WFM) and in the order of meters, say 5 m, in the inversion step (WFI), meaning that depth layer (z_{m-1}, z_m) is subdivided in a

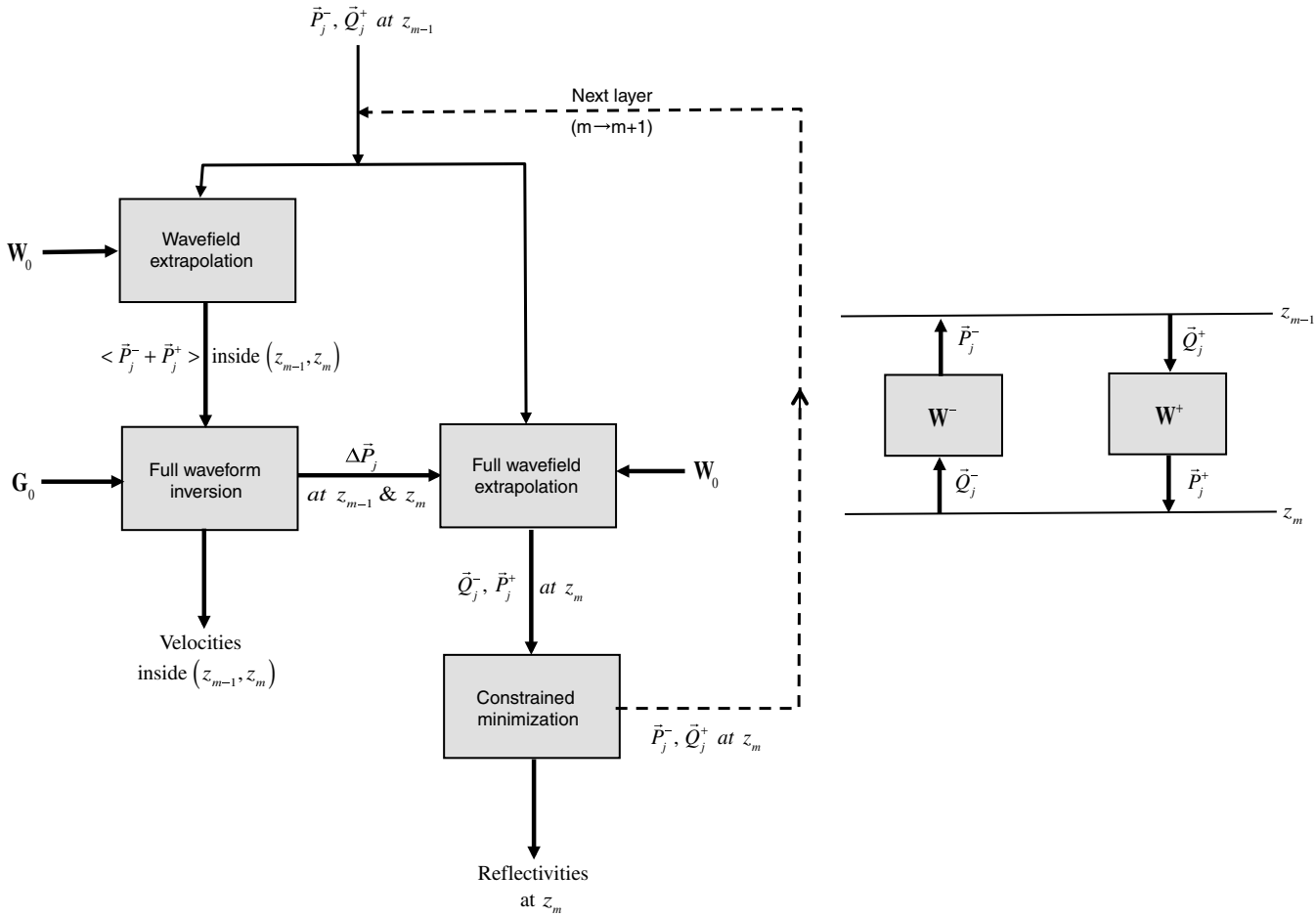

Figure 5. JMI combines WFM and WFI into a recursive joint migration-inversion process. WFM estimates the wavefields by full wavefield extrapolation, and WFI updates the wavefields and computes the velocities by full waveform inversion. The output yields reflectivity and velocity, optionally at different scales.

set of mini-layers with thickness δz_m. The double scale JMI process will be of particular interest in reservoir areas, where detail in the order of meters is required. Including broadband interbed multiples is considered to be essential in providing that degree of detail.

Figure 5 illustrates the computational diagram of JMI, being a combination of Figures 3 and 4, and showing the alternate application of the WFM and WFI process at each depth level. The output equals angle-dependent reflection coefficients (Radon transform of $\vec{R}_k$) and angle-dependent velocities (Radon transform of $\vec{\chi}_k$) at each gridpoint. Note also that in the simplest implementation, the WFM step is applied with current migration technology, meaning that in the computation of the wavefields primary reflections are addressed only ($\mathbf{R}^{\cap}$ is ignored). Of course, the WFI step always involves the multiple scattering process in layer (z_{m-1}, z_m) because velocity is very nonlinear in the seismic data.

CONCLUSIONS

Current seismic migration has been extended to the concept of WFM, allowing the utilization of surface and interbed multiple scattering without user involvement. In addition, in WFM the familiar imaging principle is replaced by a constrained minimization process at each depth level.

Similarly, current seismic inversion has been extended to the concept of WFI, allowing also the utilization of surface and interbed multiple scattering without user involvement. In addition, in WFI the familiar minimization process at the surface is replaced by a minimization process at each depth level.

It is shown that the underlying mathematical equations of WFM and WFI have an equal mathematical structure, but the physical meaning of these equations is very different.

In WFM, the equations describe a physical scattering process ($\boldsymbol{A}$-scattering). The difference in amplitude between reflected and incident wavefields determines the reflectivity in each scatter point.

In WFI, the equations describe a virtual scattering process ($\boldsymbol{B}$-scattering). The difference in traveltime between simulated and true wavefields determines the velocity in each scatter point.

By analogy with what has already been introduced in migration — extending the migration result to angle-depended reflectivity in each gridpoint — the theory of full waveform inversion has been extended to angle-dependent velocity in each gridpoint. With this extension, WFI can extract anisotropy from seismic data in a data-driven manner.

I propose that we use WFM and WFI in one recursive joint migration-inversion process, being referred to as JMI. In this recursive process the elaborate volume integral solution is replaced by an efficient alternative: WFM and WFI are alternately applied at each depth level, where WFM estimates the incident wavefields by full wavefield extrapolation and WFI updates the incident wavefields and computes the velocities by full waveform inversion. The output is two-fold, consisting of an angle-dependent reflectivity image and an anisotropic velocity model, optionally at different scales.

The amount of seismic data that we acquire increases exponentially and follows Moore's law. This means that if we want to keep the number of experts in the seismic value chain the same, then the working hours per megabyte must be decreased. This productivity challenge can be met if user-intensive processes in processing and interpretation are automated to a large extent. In this respect, we may expect that the proposed joint migration-inversion process — where velocity models are determined and multiples are used without user interaction — will have a large strategic value for the industry.

ACKNOWLEDGMENTS

The author would like to thank the Delphi sponsors for the stimulating discussions and their financial support.

REFERENCES

Abubakar, A., W. Hu, T. M. Habashi, and P. M. van den Berg, 2009, Application of the finite-difference contrast-source inversion algorithm to seismic full-waveform data: Geophysics, **74**, no. 6, WCC47–WCC58, doi: 10.1190/1.3250203.

Beasley, C. J., R. E. Chambers, and Z. Jiang, 1998, A new look at simultaneous sources: 68th Annual International Meeting, SEG, Expanded Abstracts, 133–135.

Berkhout, A. J., 1982, Seismic migration, imaging of acoustic energy by wavefield extrapolation, second edition: Elsevier.

Berkhout, A. J., 1984, Multidimensional linearized inversion and seismic migration: Geophysics, **49**, 1881–1895, doi: 10.1190/1.1441601.

Berkhout, A. J., 1997, Pushing the limits of seismic imaging, Part II: integration of prestack migration, velocity estimation and AVO analysis: Geophysics, **62**, 954–969, doi: 10.1190/1.1444202.

Berkhout, A. J., and D. J. Verschuur, 1994, Multiple technology, Part 2: Migration of multiple reflections: 64th Annual International Meeting, SEG, Expanded Abstracts, 1497–1500.

Claerbout, J. F., 1976, Fundamentals of geophysical data processing: McGraw-Hill.

Gisolf, A., and D. J. Verschuur, 2010, The principles of quantitative acoustic imaging: Houten, EAGE.

Stolt, R. H., and A. B. Weglein, 1985, Migration and inversion of seismic data: Geophysics, **50**, 2458–2472, doi: 10.1190/1.1441877.

Symes, W. W., 2008, Migration velocity analysis and waveform inversion: Geophysical Prospecting, **56**, 6, 765–790, doi: 10.1111/gpr.2008.56.issue-6.

Tarantola, A., 1987, Inverse problem theory, methods for data fitting and model parameter estimation: Elsevier.

Virieux, J., and S. Operto, 2009, An overview of full waveform inversion in exploration geophysics: Geophysics, **74**, no. 6, WCC127–WCC152, doi: 10.1190/1.3238367.

Whitmore, N. D., A. A. Valenciano, and W. Sollner, 2010, Imaging of primaries and multiples using a dual-sensor towed streamer: 80th Annual International Meeting, SEG, Expanded Abstracts, 3187–3192.

Zhdanov, M. S., 2002, Geophysical inverse theory and regularization problems: Elsevier.